Original Investigations

Deep Structure of the Southern Rhinegraben Area from Seismic Refraction Investigations*

J. B. Edel**

Institut de Physique du Globe, Strasbourg

K. Fuchs, C. Gelbke, C. Prodehl

Geophysikalisches Institut der Universität Karlsruhe

Abstract. A joint interpretation of all seismic-refraction profiles in the southern part of the Rhinegraben area is presented. A time-term analysis of all P_g-arrivals reveals the topography of the crystalline basement and provides an average velocity of 6.0 km/s for the uppermost crust. The crust-mantle boundary is clearly elevated in the Rhinegraben rift system forming an arch with a span of 150—180 km and reaching a depth of only 25 km at the flanks of the graben proper. The velocity of P-waves in the uppermost mantle is 8.0—8.1 km/s. Below the flanks of the graben, the crust-mantle boundary is formed by a first-order discontinuity. Within the graben proper it is replaced by a transition zone of 4 km thickness with the strongest velocity gradient at a depth of 21 km. This transition zone is regarded as region of crust-mantle interaction and seems to be confined to the graben proper.

Key words: Seismic-Refraction Profiles — Rhinegraben — Time-Term Analysis — Elevation of Crust-Mantle Boundary — Crust-Mantle Transition

Introduction

Since the large explosions near Haslach in the Black Forest in 1948 (HA in Fig. 1) the Rhinegraben, especially its southern part, has been the site of a large number of explosion-seismic experiments (Fig. 1 and Table 1). Also deep-reflection profiles were recorded in some areas of the Rhinegraben (Dohr, 1957, 1967, 1970; Schulz, 1957). The explosions during one of these experiments (near Rastatt, 1971) could be used for seismic-refraction observations (profile RA-250). These investigations culminated in a large-scale refraction survey in September 1972 in the southern part of the Rhinegraben when a dense network of seismic-refraction profiles was established (Rhinegraben Research Group, 1974; Fig. 1).

It is the purpose of this paper to present a unified interpretation of all available deep-seismic sounding data in the southern part of the Rhinegraben. Strong lateral variations in the uppermost crust cause difficulties in their interpretation. The geological and tectonic structure of the area under investigation is extremely complex. Three main tectonic events have influenced the area: The Variscan orogeny mainly in
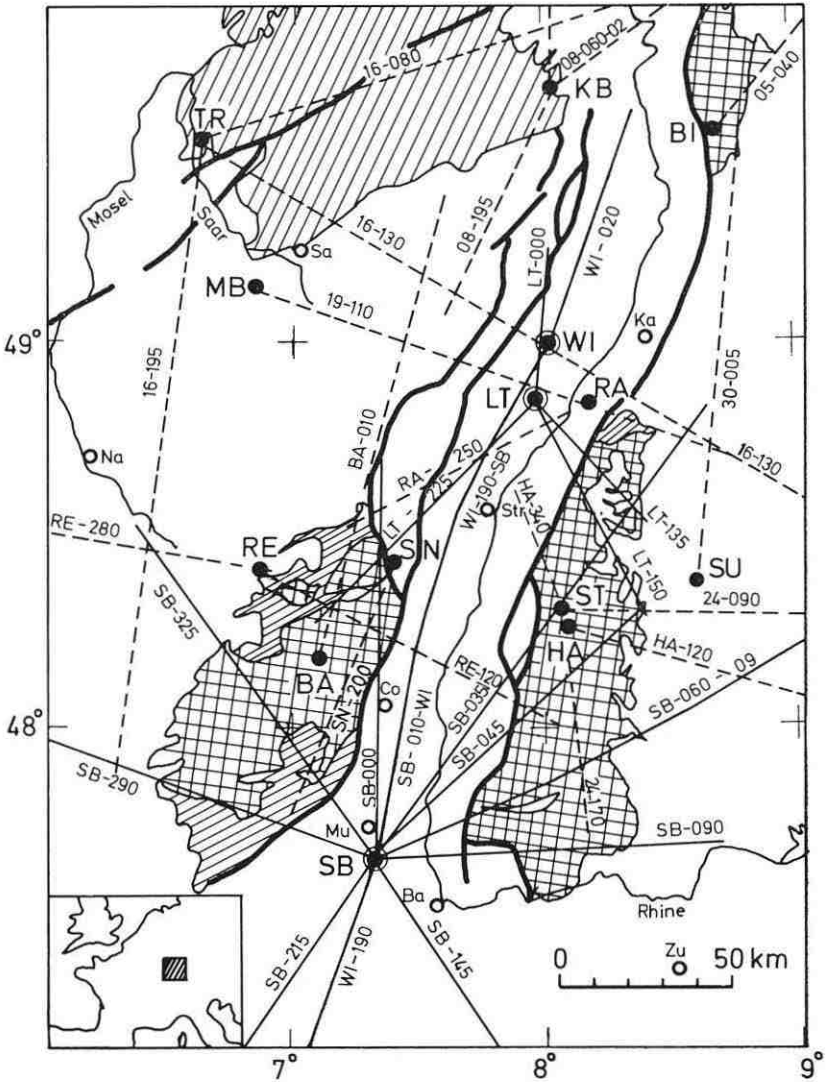
Fig. 1. Location map of seismic-refraction profiles in the central and southern Rhinegraben until 1974

Explanations:

⊙———————   profiles recorded in September 1972

● — — —   other profiles

Each profile is denoted by: shotpoint code — azimuth (—reversed shotpoint code)

▬▬▬▬▬   faults

⊞⊞⊞⊞   crystalline outcrops

▨▨▨▨   Paleozoic outcrops

Fig. 1. Explanations: (continued)

⊙ ●   Shotpoints:

LT	Leutenheim,	SB	Steinbrunn,
WI	Wissembourg,	BA	Col des Bagenelles,
HA	Haslach,	BI	Birkenau (05[a]),
MB	Merlebach,	KB	Kirchheim-
RE	Raon l'Étape,		bolanden (08),
ST	Steinach (24),	SN	Saint Nabor,
TR	Taben Rodt (16)	SU	Sulz (30)

○   Cities:

Ba	Basel	Na	Nancy
Co	Colmar	Sa	Saarbrücken
Ka	Karlsruhe	Str	Strasbourg
Mu	Mulhouse	Zu	Zürich

[a] The numbers refer to the denotations used for shotpoints (quarries) within western Germany (Bamford, 1973; Giese and Stein, 1971).

Table 1. Profiles observed prior to 1972 and references

Shotpoint	Azimuth	Profile[a]	Authors of Interpretations[b]
Haslach (HA)	120	HA-120	1, 2, 3, 4, 5, 6, 7, 12, 14, 15, 16, 17, 18, 19
Haslach (HA)	340	HA-340	2, 5, 12, 16, 17, 18, 19
Taben-Rodt (TR)	080	16-080	6, 9, 10, 11, 17
Taben-Rodt (TR)	130	16-130	1, 2, 3, 6, 12, 13, 14, 17
Taben-Rodt (TR)	195	16-195	2, 14, 17
Merlebach (MB)	110	19-110	1, 2, 6, 12, 13, 14, 17
Kirchheimbolanden (KB)	195	08-195	2, 17
Saint Nabor (SN)	200	SN-200	1, 2, 3, 6, 8, 13, 14, 17
Col des Bagenelles (BA)	010	BA-010	1, 2, 3, 6, 8, 13, 14, 17
Raon l'Étape (RE)	120	RE-120	2, 14, 17
Raon l'Étape (RE)	280	RE-280	2, 14, 17
Birkenau (BI)	040	05-040-02	3, 5, 6, 11, 17
Rastatt (RA)	250	RA-250	2, 17
Steinach (ST)	090	24-090	2, 3, 14, 17
Steinach (ST)	170	24-170	1, 2, 3, 14, 17

[a] The denotation corresponds to that by Giese and Stein (1971).

[b] 1 Ansorge et al. (1970), 2 Edel et al. (this report), 3 Emter (1971), 4 Förtsch (1951), 5 German Research Group (1964), 6 Giese and Stein (1971), 7 Landisman and Mueller (1966), 8 Lauer and Peterschmitt (1970), 9 Meissner and Berckhemer (1967), 10 Meissner et al. (1970), 11 Meissner and Vetter (1974), 12 Mueller et al. (1967), 13 Mueller et al. (1969), 14 Mueller et al. (1973), 15 Prodehl (1965), 16 Reich et al. (1948), 17 Rhinegraben Research Group (1974), 18 Rothé (1958), 19 Rothé and Peterschmitt (1950).

NE-SW direction, the Alpine orogeny causing a general uplift and block faulting of the Variscan area, and the formation of the graben. In consequence, the sedimentary covers show variable thicknesses: reaching 6000 m in the "Saar-Nahe-Trog" in the NW, 2000—4000 m in the graben, while in other areas (Vosges, Black Forest, Odenwald) the crystalline basement is exposed. — Special explosions in drill holes are expensive and could be arranged only in a few cases. Otherwise, available quarry blasts had to be used as energy sources. Therefore, the position of the profiles is not always optimal with regard to geologic and tectonic settings of the area.

In spite of these complications the record sections of the numerous profiles exhibit a similar pattern of traveltime branches which permit a classification of the observed record sections in relation to the graben. Conventional flat-layer methods of interpretation had to be applied with care. They were supplemented by a time-term analysis for the top of the basement.

Correlation of Phases

Most of the data obtained in the area of investigation are presented in record sections (Figs. 2—6). The correlated traveltime curves are shown in the record sections by thin dashed lines. Lateral heterogeneities are expressed clearly in breaks and sudden delays of the traveltime curves which can be correlated frequently with tectonic and petrographic changes. This makes the correlation sometimes very difficult. The size of the relative amplitudes varies considerably within one profile as well as from one profile to the other. In some cases, multiple phases can be identified in the distance range from 0 to 60 km (e. g. profile WI-190-SB).

The general pattern of traveltime curves of all record sections (Fig. 7) corresponds to a general velocity-depth model (see Fig. 11), the variations of which do not only cause traveltime delays but also significant changes of relative amplitudes.

First Arrivals. Only within the first 10 km the direct wave travelling in the sediments (P_s) is visible. The P_g-arrivals can be followed in the distance range from 10 to 60 km and for some profiles up to 90 km. The P_n-phase can be correlated only on part of the profiles as first arrival at distances greater than 90 km (Table 2). The only reversed profile in the area under investigation is that between Steinbrunn (SB) and Wissembourg (WI). The scatter of P_n-arrivals on the record sections of this line causes difficulties in the exact determination of the true velocity within the uppermost mantle. Nevertheless, the data indicate that the true P_n-velocity is about 8.0—8.1 km/s.

Reflected Phases. On the profiles in the central part of the Rhinegraben (16—130, 16—195, 19—110, 08—195, WI—120) reflections within the upper crust are well developed (phases 3, 4). The relative amplitudes of phase 1 ($P_M P$-reflection) and phase 2 (intermediate reflection from the lower crust) seem to vary from region to region. In the southern graben proper (profiles SB-035, SB-010-WI, SB-000, WI-190-SB, RA-250) phase 2 is dominant. Here the $P_M P$-reflection is either hidden within the coda of the high-amplitude phase 2 or is too weak. On the profiles crossing the flanks of the graben, however, mostly the $P_M P$-reflection shows the strongest amplitudes (phase 1), while the reflected phase 2 is less well developed (SB-060-09, SB-045, 24-090, 24-170, 05-140-02, LT-225, BA-010, SN-200, RE-280). On some profiles (RE-120, SB-290) crustal reflections (phase 2, 3) and $P_M P$ (phase 1) are both well
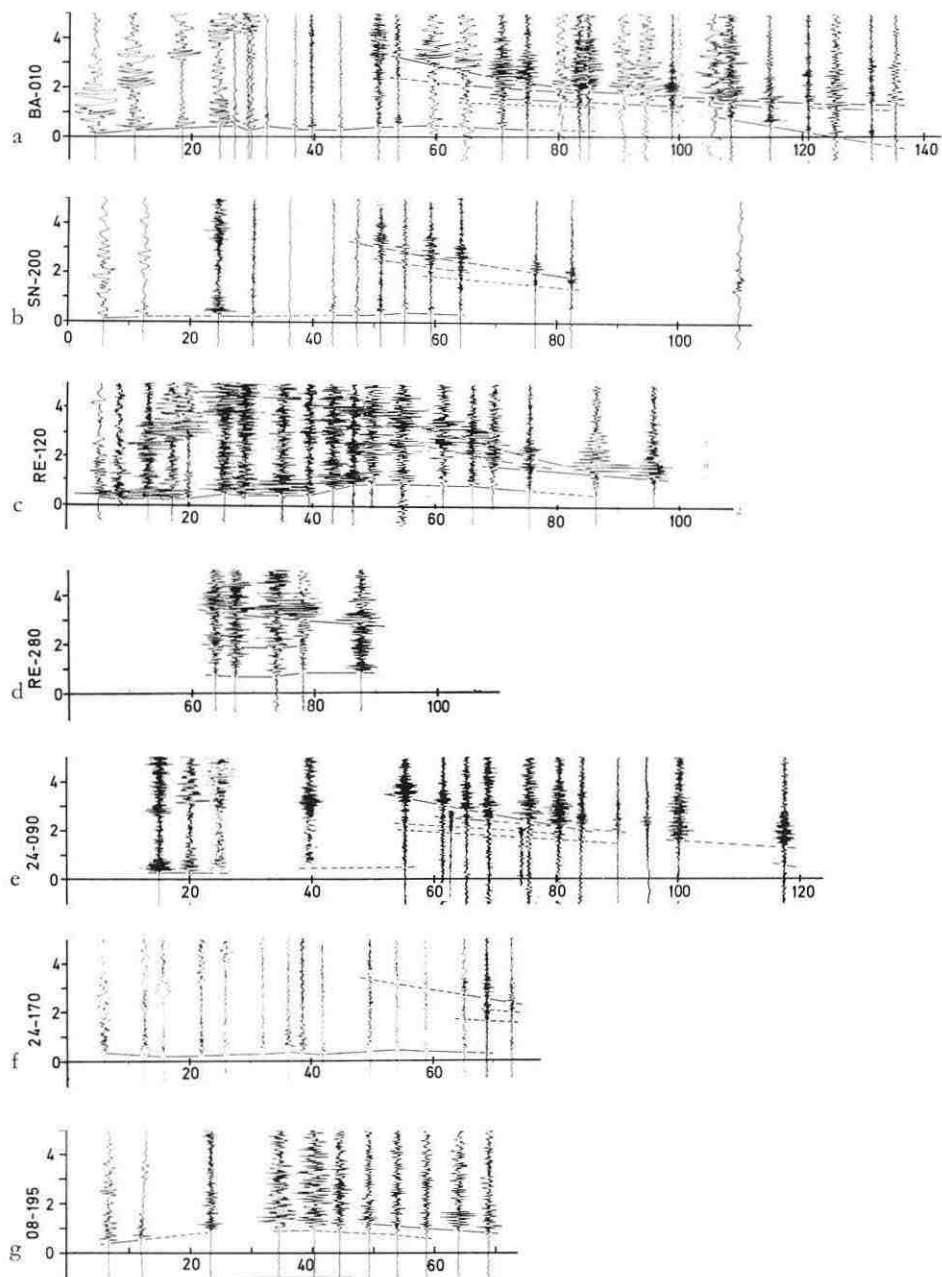
Fig. 2a–g. Record sections. From top to bottom: Bagenelles-N (BA-010), Saint Nabor-S (SN-200), Raon l'Étape-ESE (RE-120), Raon l'Étape-W (RE-280), Steinach-E (24-090), Steinach-S (24-170), Kirchheimbolanden-S (08-195)
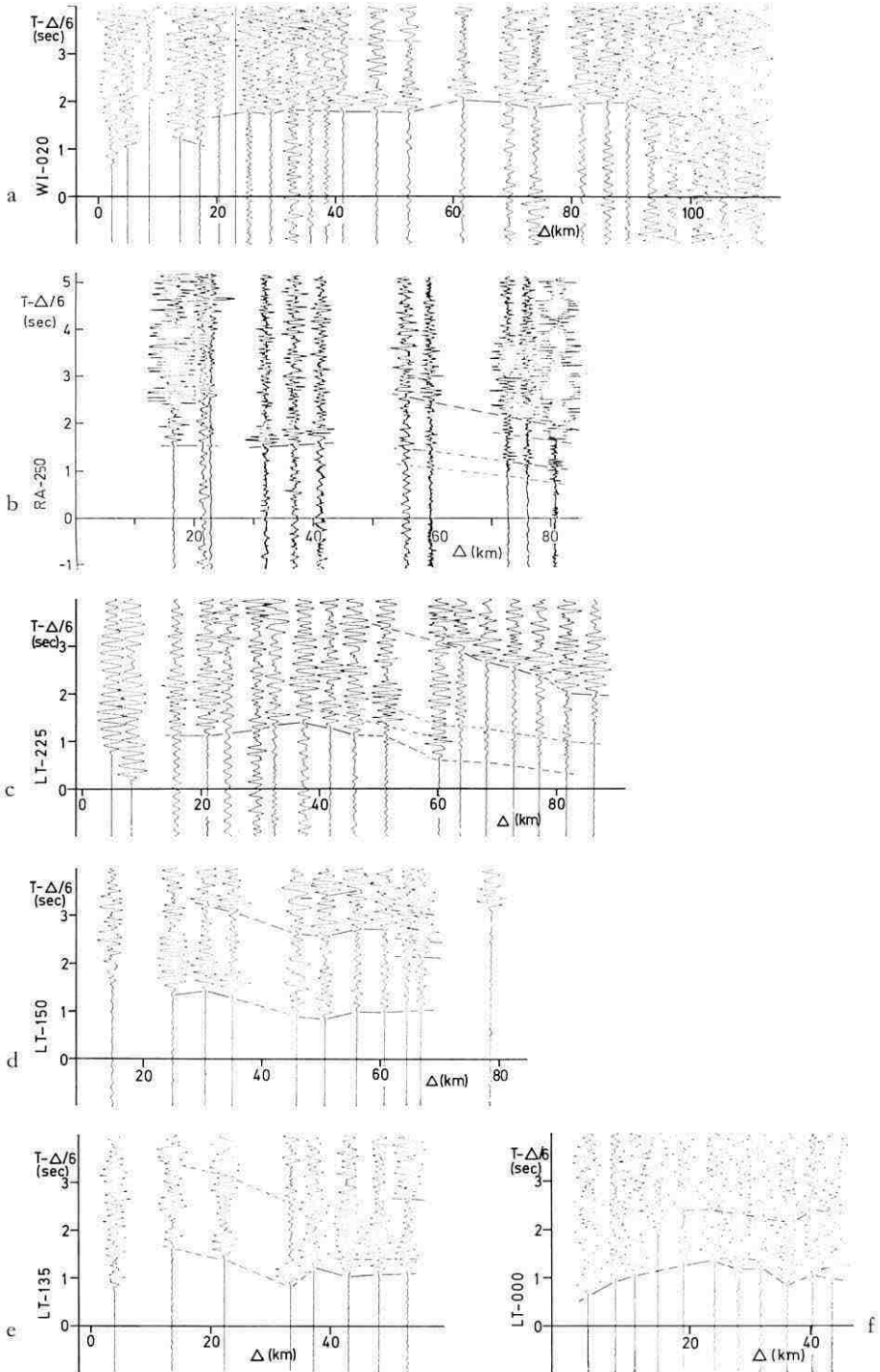
Fig. 3a–f. Record sections. From top to bottom: Wissembourg-N (WI-020), Rastatt-SW (RA-250), Leutenheim-SW (LT-225), Leutenheim-SSE (LT-150), Leutenheim-SE (LT-135), Leutenheim-N (LT-000)
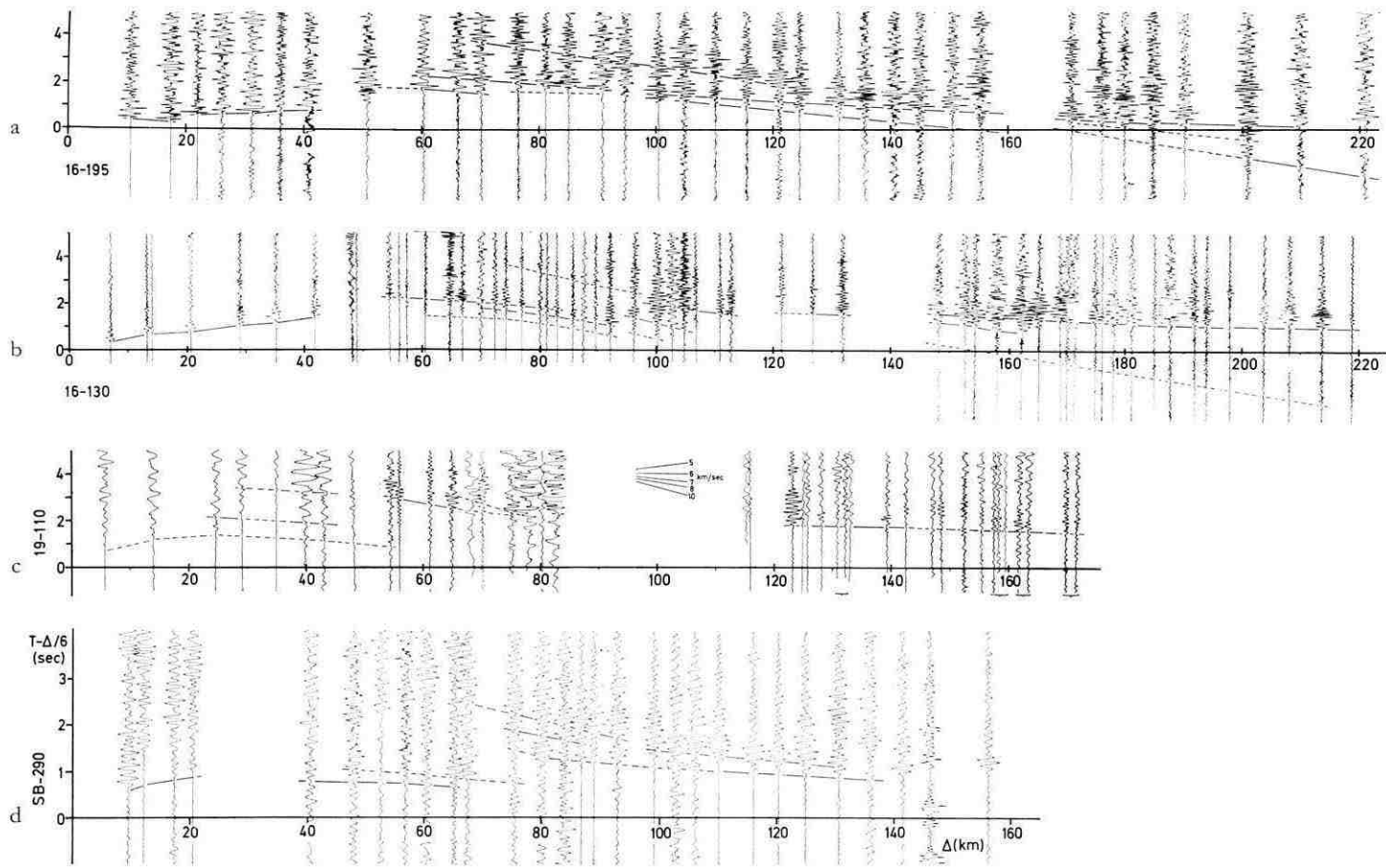
Fig. 4a–d. Record sections. From left to right: Taben Rodt-S (16-195), Taben Rodt-ESE (16-130), Merlebach-E (19-110), Steinbrunn-W (SB-290)
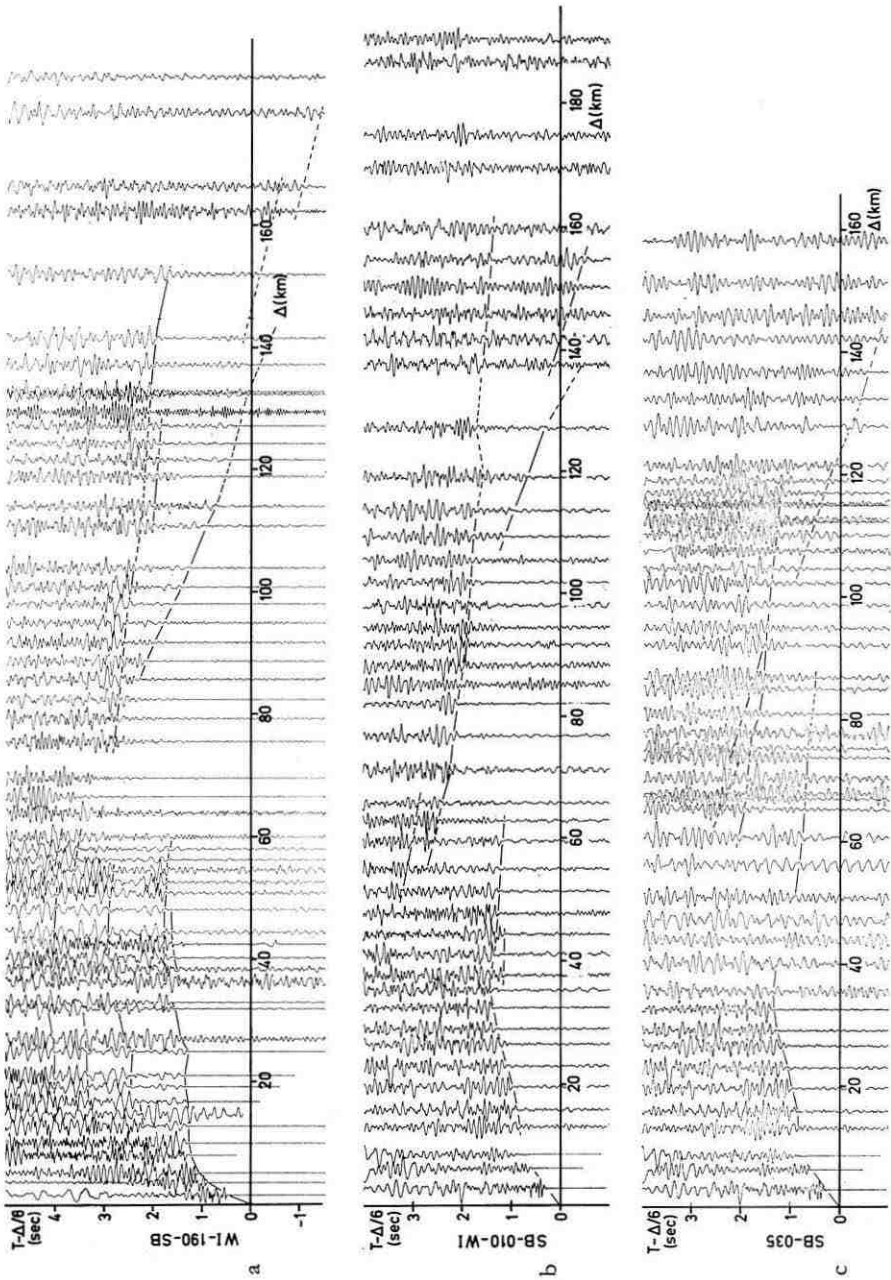
Fig. 5a–c. Record sections. From left to right: Wissembourg-S (WI-190-SB), Steinbrunn-N (SB-010-WI), Steinbrunn-NNE SB-035)
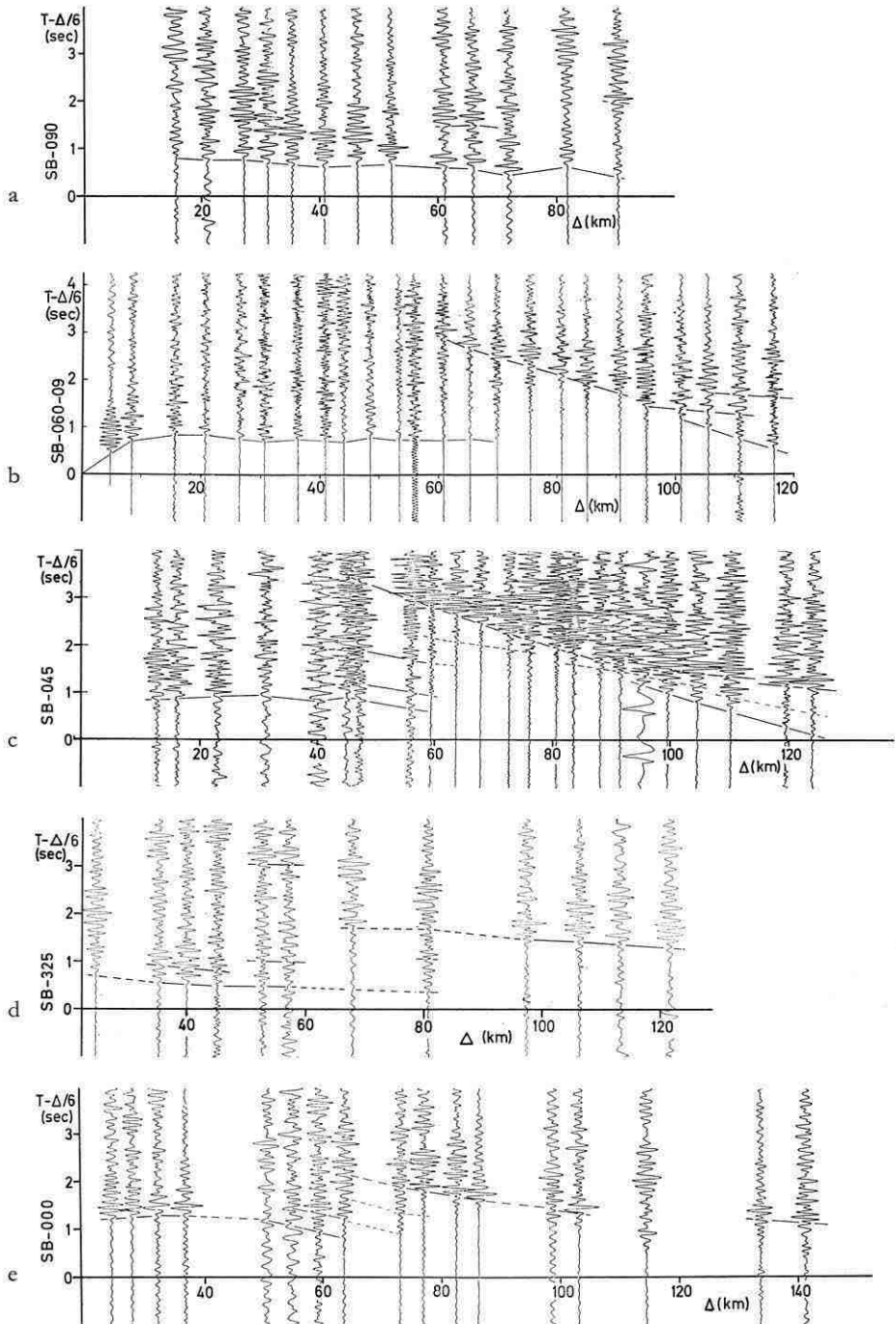
Fig. 6a—e. Record sections. From top to bottom: Steinbrunn-E (SB-090), Steinbrunn-ENE (SB-060-09), Steinbrunn-NE (SB-045), Steinbrunn-NW (SB-325), Steinbrunn-NNW (SB-000)
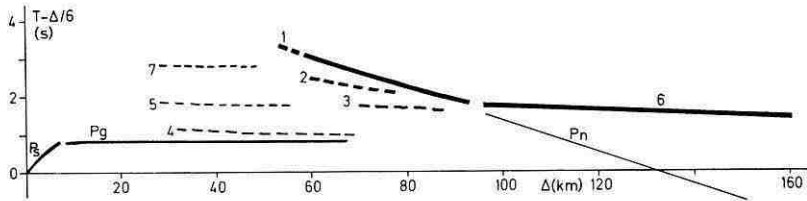
Fig. 7. Basic traveltime diagram of the profiles recorded in the Rhinegraben area

Table 2. P_n observations

Profile	apparent P_n velocity (km/s)	distance range (km)
SB-060-09	7.8	95–125
	8.3	125–150
SB-045	7.9	95–125
SB-035	8.0	110–140
SB-010-WI	8.05	105–130
WI-190-SB	8.1	100–130
16-130	7.8	160–195
16-195	7.8	170–210

expressed. Phase 6 in Fig. 7 denotes strong arrivals which are observed beyond 100 km distance. In the preliminary interpretation by Rhinegraben Research Group (1974) these arrivals were erroneously interpreted as $P_M P$ phase. However, in a more detailed analysis that correlation had to be modified to take into account the existence of phases 2 and/or 3 and a sharp bend in the traveltime curve with an abrupt change in apparent velocity (SB-045, BA-010, RE-120, SB-290): The phase 6 has rather to be interpreted as formed by supercritically reflected energy of the phases 2 and/or 3. The record sections also show that not only supercritically reflected energy is recorded, but also energy is visible in the subcritical distance ranges. In some cases, phases denoted as 4, 5, and 7 can be recognized between 20 and 60 km which apparently continue phases 2 or 3 to smaller distances. While phases 5 and 7 could be identified as multiple reflections from the free surface, phase 4 is probably caused by a heterogeneity in the upper part of the crystalline basement. These phases have not been included in the determination of the velocity-depth model.

Inversion of Observations

The strong lateral heterogeneities in the area under investigation complicate the determination of a detailed velocity-depth distribution, since most of the existing inversion methods require the absence of lateral variations.

The basement delays in the sediments and the velocity in the crystalline basement can be estimated by applying a time-term method (Bamford, 1973) to the numerous P_g-observations. Taking the velocity in the bottom layer as constant this "refractor" velocity is 6.00 ± 0.02 km/s. Fig. 8 shows the contours of the delay times in the area
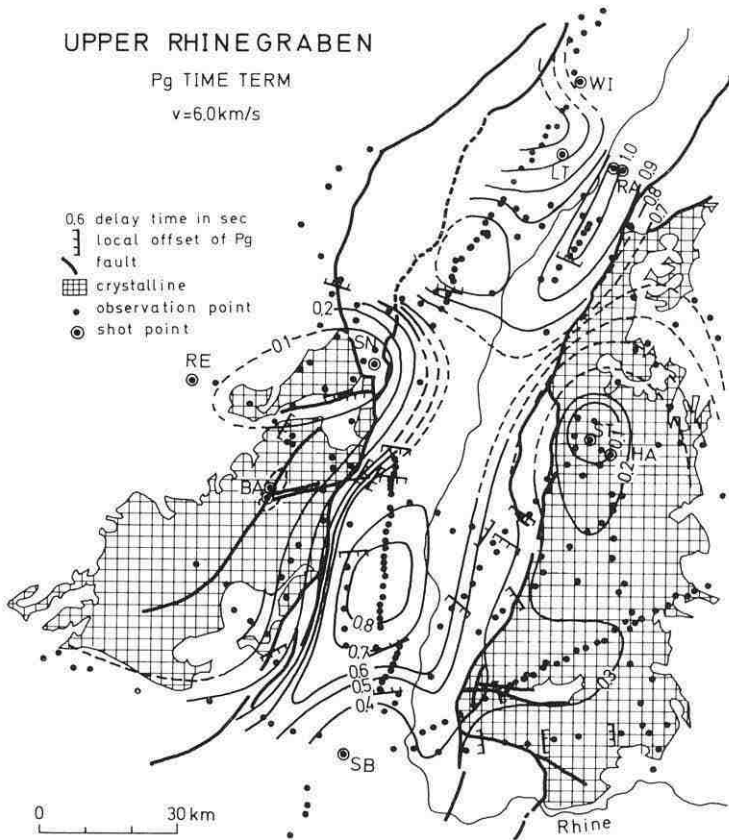
Fig. 8. Delay-time map of the 6.0 km/s surface for the upper Rhinegraben based on fourth order Fourier series solutions. Cross-hatched areas represent crystalline and Paleozoic outcrops. Shotpoint codes see Fig. 1

as computed for a surface formed by a first-order polynomial and fourth-order Fourier series. The conversion of these delay times into depths of the top of the 6 km/s-layer was not performed because the large variations of the overburden velocity are not known sufficiently.

The contour lines in the graben reflect in a first approximation the variations of the depth to the basement. Two great depressions are evident: the southern one between Mulhouse and Colmar in the potash basin of Alsace, the northern one in the so-called "Rastatter Loch" between Baden-Baden and Karlsruhe. Relatively low values of delay times are obtained in the south on the horst of Mulhouse and in the middle of the map on the swells of Colmar and Erstein. The delay times in the areas of outcropping basement are small, but vary slightly, possibly due to the fact that the influence of weathering and fracturing changes from one area of the basement to the other. Sudden delays in the P_g-traveltime curves, possibly caused by vertical displacements of the basement, are also indicated in the map.

Contour Map of the Crust-Mantle Boundary. The depth of the crust-mantle boundary is derived from all observed data of phase 1 in the distance range from 50—90 km.
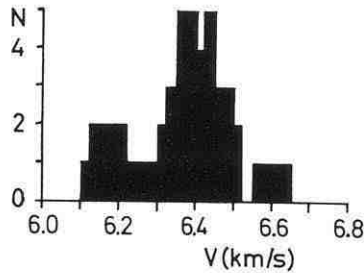
Fig. 9. Histogram showing average crustal velocity vs. frequency of occurrence (number N of profiles) as determined by the T^2, Δ^2 method for the southern and central Rhinegraben

The average crustal velocity on each profile is estimated by the T^2, Δ^2 method. The observations have been corrected to a reference level at a depth of 3 km taking into account sediments or basement rocks as described in detail by Rhinegraben Research Group (1974). From the histogram of the average crustal velocities of all profiles (Fig. 9) 6.4 km/s appears to be a representative velocity. To take into account the effect of ray refraction (e.g., Dix, 1955; Stewart, 1966) the smaller value of 6.25 km/s was then chosen for depth-calculations in a single-layer crust as mean crustal velocity below the reference depth of 3 km. Even then the average velocity is relatively high. It must partly be attributed to the elimination of the uppermost 3 km; but may also be partly connected with the existence of high velocities (about 7 km/s) in the lower crust as will be shown below. Depth values derived from seismic-reflection data (Demnati and Dohr, 1965; Dohr, 1967, 1970) with the same mean crustal velocity have been included in the contour map (Fig. 10) showing depths below sea level. Assuming 8.0—8.1 km/s as true velocity, the dip deduced from the observed apparent P_n-velocities (Table 2) is concordant with the topography of the crust-mantle boundary based on the reflected phase 1 ($P_M P$).

Slight differences between this contour map and the one presented earlier by Rhinegraben Research Group (1974) are due to the restriction on the reliable observations of phase 1 in this paper. The crust-mantle boundary is clearly elevated in the area of the Rhinegraben rift system reaching a minimum depth of 24—25 km in its southern part. The dome-like elevation displays slight asymmetry: its slope towards the east is rather gentle while towards the northwest and south it is rather steep.

Detailed Velocity-Depth Models. From the main phases shown in Figs. 2—6, for each profile a starting model is derived applying the T^2, Δ^2 method or intercept-time formulas, etc. In a second stage this model is improved by comparison of theoretical and observed traveltimes and position of critical points. This step is done iteratively until the best fit is reached. Then the observations are compared with theoretical seismograms in order to obtain not only the best fit of traveltimes but also of relative amplitudes of the different phases.

The generalized traveltime correlation of Fig. 7 is concordant with the following generalized velocity-depth model depicted in Fig. 11. The velocity in the surface layer (sediments and weathered basement rocks) has been roughly estimated as 4.0 km/s, for the depth range AB a constant average velocity of 6.0 km/s is taken from the time-
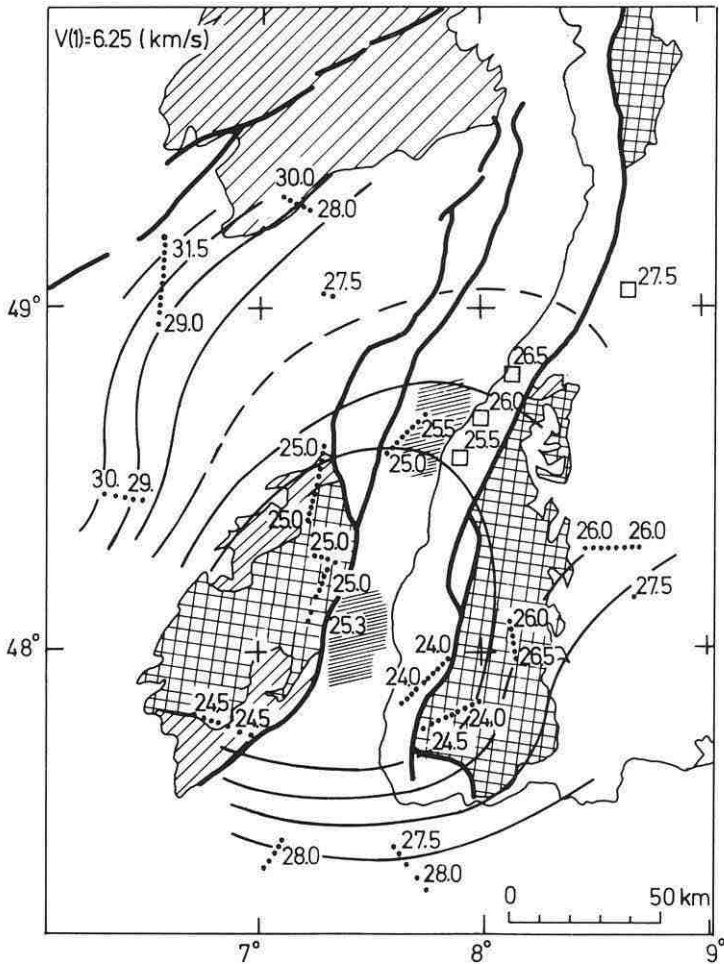
Fig. 10. Contour map of the depth to the crust-mantle boundary below sea-level for the area of the southern Rhinegraben (based on phase 1). The depths are calculated with a mean crustal velocity V (1) = 6.25 km/s below a reference depth of 3 km

28.8	depth in km
••••••••	positions for which depths were calculated from seismic-refraction data
□	positions for which depths were calculated from seismic-reflection data
////	areas where phase 1 is not observed

Further explanations see Fig. 1

term method. It is difficult to deduce details of the velocity-depth structure in this depth range, though, locally, the true P_g-velocity may be higher or lower than 6.0 km/s. Especially, a zone of low velocity has not been included in the generalized velocity-depth distribution between A and B. Such a velocity inversion had been deduced in the area of the Rhinegraben from previous observations by a number of
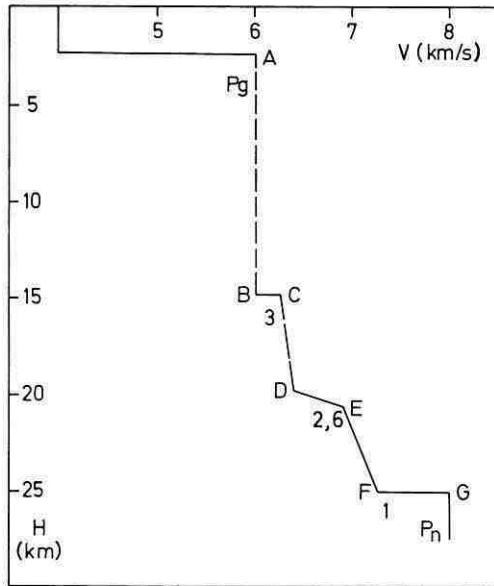
Fig. 11. Generalized velocity-depth model for the area of the Rhinegraben. Explanations of A, B, C, ... see text. P_g, P_n, 1, 2, 3: denotation of depth ranges from which the corresponding phases in the traveltime diagram (see Fig. 7) originate

authors (Ansorge *et al.*, 1970; Meissner *et al.*, 1970; Meissner and Vetter, 1974; Mueller *et al.*, 1967, 1969, 1973). The phase corresponding to the reflection from the bottom of such a low-velocity zone was termed P_c by Mueller and Landisman (1966). Although such a phase can be found on some profiles it is often impossible to follow it to neighbouring profiles and map it on a regional scale. The new observations of 1972 furnished no further information concerning the low-velocity zone. The explosions within the graben proper generated strong multiple reflections and reverberations within the sediments which completely mask the distance range important for the detection of P_c. Therefore, no fine structure was included in the upper part AB of the crustal model, and only its average velocity was taken into account. The presence of considerable vertical and horizontal heterogeneities in this zone is quite likely, and is indicated by the dashed line. A more complicated velocity-depth distribution in this range, however, would only little affect the model derived for the structure of the middle and lower crust (see Fig. 14).

The reflections from the transition zones BC, DE, FG are formed by phases 3, 2, and 1, respectively. Their relative amplitudes are governed by the velocity increase and the thickness of the transition zone which are found to be different inside and outside of the graben. The following examples demonstrate clearly this important difference.

On the record section of the profile SB-010-WI (Steinbrunn to Wissembourg) in Fig. 12, completely located in the graben proper, phases 1 and 3 are absent, and P_n is intersecting phase 2 reflected from zone DE at a depth of about 20 km. In the graben proper this zone has the strongest velocity gradient and produces the predominant reflection from the lower crust. The first-order discontinuity at FG has
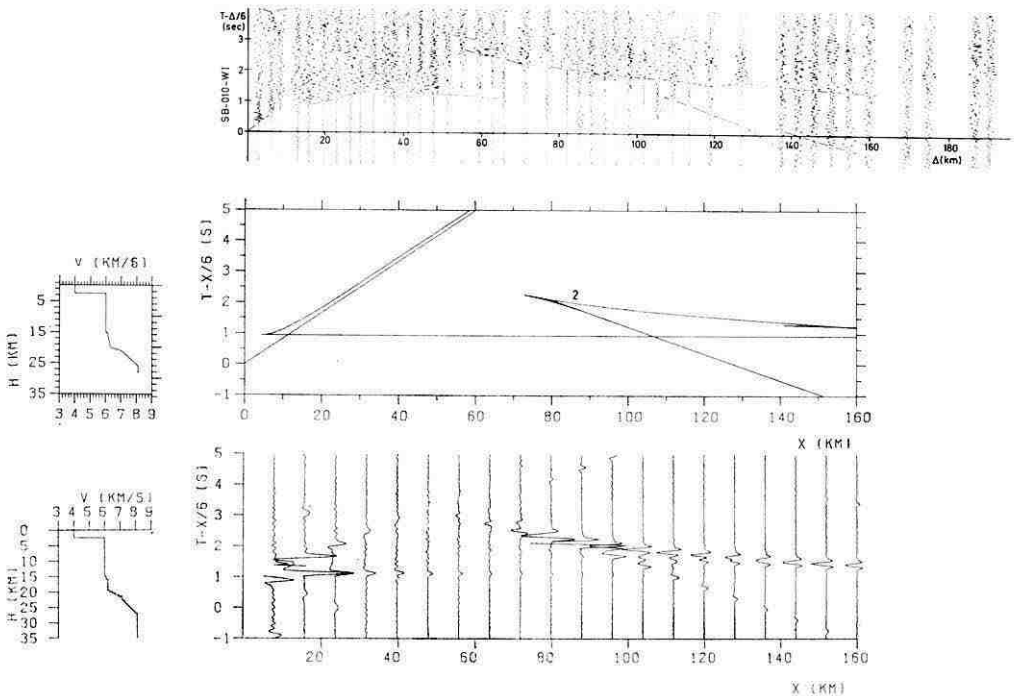
Fig. 12. Observed record section, traveltime interpretation, and synthetic record section of profile SB-010-WI with the corresponding velocity-depth functions

disappeared. The transition zone EF merges continuously into the upper mantle generating the relatively strong P_n-amplitudes. The velocity step at BC is also smaller than outside the graben proper.

The profile SB-045 (Steinbrunn-NE) crosses the eastern flank of the Rhinegraben. On the record section of this profile (Fig. 13) P_n is tangential to phase 1 which here provides the prominent arrivals. The reflecting zone FG is formed by a first-order discontinuity. Phase 2 is best recognized by the abrupt change of the apparent velocity of the large-amplitude reflections at 90 km distance, its critical point being located close to the intersection of phases 1 and 2.

The record section of profile BA-010 (Bagenelles-N) in Fig. 14 (top) displays a very similar amplitude pattern of the phases 1 to 3 compared with profile SB-045. P_n is again tangential to phase 1 and phases 1 and 2 are intersecting close to the critical point of phase 2. On this profile phase 3 can be traced backwards to a distance of at least 70 km. It must be regarded as phase P_c reflected from the bottom of a low-velocity zone within the upper crust. For comparison, Fig. 14 contains synthetic record sections for two crustal models which differ in the presence of a low-velocity zone in the upper crust. Phases 1 and 2 duplicate the observations satisfactorily and are little influenced by the different structure of the upper crust. Phase 3 is better explained by the presence of a low-velocity zone.

It should be pointed out that the observed and the synthetic record sections indicate the existence not only of supercritically but also of subcritically reflected energy which is already visible 10—20 km prior to the critical distance.
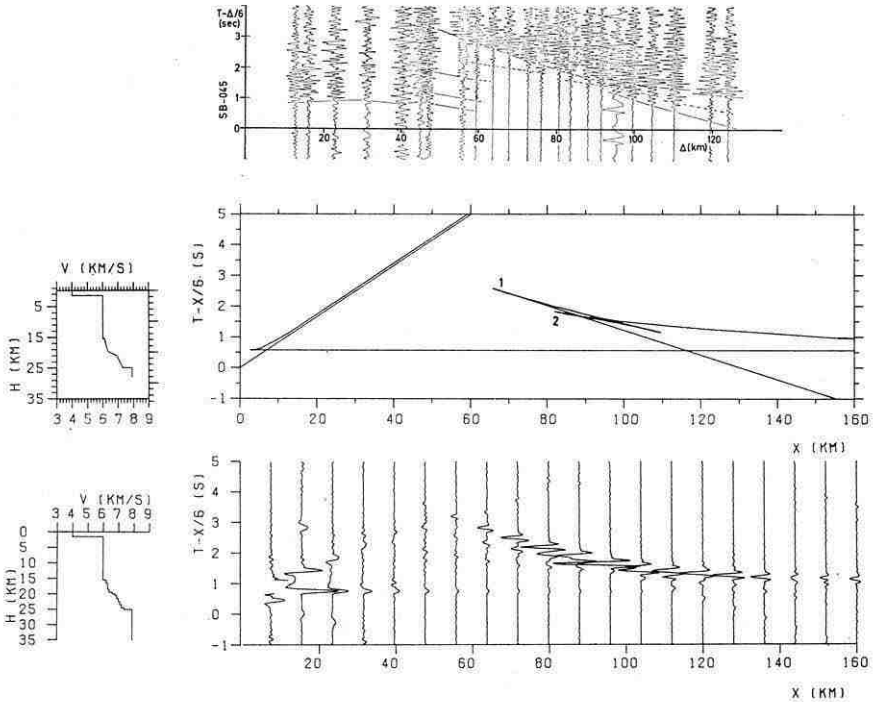
Fig. 13. Observed record section, traveltime interpretation, and synthetic record section of profile SB-045 with the corresponding velocity-depth functions

Detailed velocity-depth models are also derived for all other profiles in the southern part of the Rhinegraben rift system wherever an interpretation in terms of negligible lateral heterogeneity is justified. A compilation of these models is discussed in the next section.

Crustal Structure in the Southern Part of the Rhinegraben Rift System

In Fig. 15 an attempt has been made to compile selected crustal models (Table 3) derived in various parts of the southern Rhinegraben. The inlets with the models are placed as close as possible into the regions of which they are typical. As pointed out already a systematic regional variation related to the graben proper can be recognized.

Outside the graben proper all models are characterized by zone FG as a first-order discontinuity at a depth of 25—26 km where the velocity increases abruptly from about 7.3 to 8.0 km/s. Since zone FG is also the zone of the strongest gradient, there should be no dispute that it represents the crust-mantle boundary. In the graben proper the strongest gradient is encountered in zone DE at a depth of about 21 km where the velocity starts to increase rapidly from 6.3 to 7.1 km/s. Below E, there is a continuous increase of velocity to 8.1 km/s, the velocity of the upper mantle. The discontinuity at FG has disappeared. In the graben proper, it is a matter of definition whether the crust-mantle boundary is placed at the depth of the strongest gradient at about 21 km (see, e. g. Giese and Stein, 1971) or at the depth between 24 and 26 km where a velocity of 8.0 km/s is reached. The authors are inclined to consider the whole
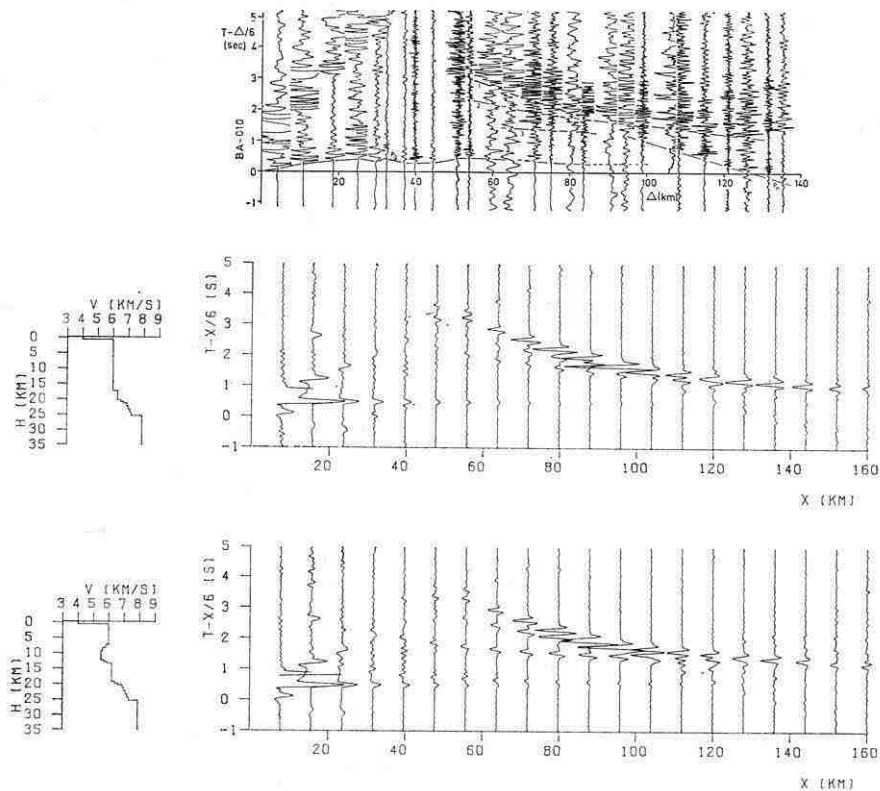
Fig. 14. Observed and synthetic record sections as determined for profile BA-010 with the corresponding velocity-depth functions

depth range between 21 and 26 km as a zone of crust-mantle interaction. This transition zone seems to be confined rather strictly to the graben proper since the first-order discontinuity FG appears as soon as profiles — originating in the graben — enter the crystalline areas of the flanks at about 60—80 km recording distance (LT-225 and SB-035). The zone DE which forms the zone of strongest gradient in the graben proper is well expressed in the neighbouring regions and separates the lower crust into two parts. Its gradient is slightly weaker outside than within the graben. In the whole area the zone BC with a velocity increase from 6.0 to about 6.2 km/s at a depth between 15 and 18 km marks the transition from the upper to the middle crust.

Two cross-sections through crust and uppermost mantle in the stripes AB and CB in the southern part of the Rhinegraben are displayed in Fig. 16. The cross-sections show lines of equal velocity (thin lines) and the depth of the main crustal boundaries (thick dashed lines) as defined by the points B, D, and F of the velocity-depth models (see Fig. 11).

The following features deserve special attention. Outside the graben proper the crust-mantle boundary is a first-order discontinuity into which the velocity isolines from 7.4—8.0 km/s converge. This boundary forms a wide arch with a span of 150—180 km rising from the west towards the graben where the 8.0 km/s-isoline reaches
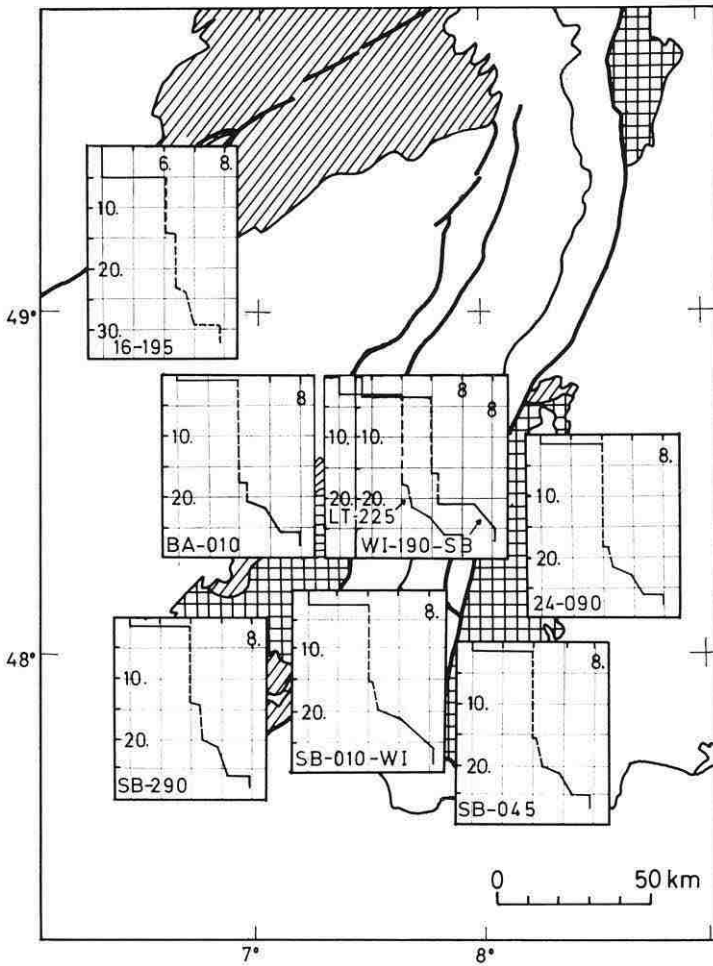
Fig. 15. Map of the area of the central and southern Rhinegraben showing velocity-depth distributions for the corresponding profiles (position see Fig. 1). The velocity-depth functions are representative for the area into which they have been placed

a depth of about 25 km. On the other side of the graben, the crust-mantle boundary dips gently towards the east. Beneath the graben proper, the first-order discontinuity near the 8.0 km/s-isoline has disappeared, here the isolines 7.2—7.8 km/s are warped upward steeply, producing a new zone of strongest velocity gradient at the shallower depth of only 21 km.

Discussion

Fig. 17 presents a compilation of the contour map for the southern Rhinegraben (Fig. 10) and the one for the northern part (Meissner and Vetter, 1974, Fig. 5). Although the number of seismic profiles in the northern part is much smaller, some common features of crustal structure can be outlined. The updoming of the mantle

Table 3. Velocity-depth models

SB-290		SB-010-WI		SB-045	
depth (km)	velocity (km/s)	depth (km)	velocity (km/s)	depth (km)	velocity (km/s)
0.0	4.0	0.0	4.0	0.0	4.0
1.5	4.0	2.5	4.0	1.5	4.0
1.5	6.0	2.5	6.0	1.5	6.0
14.0	6.0	15.0	6.0	15.5	6.0
14.5	6.3	15.0	6.1	15.5	6.1
20.0	6.4	19.5	6.3	20.0	6.3
21.0	6.9	21.0	7.0	21.0	6.9
26.0	7.2	26.0	8.1	25.0	7.4
26.0	7.9			25.0	7.9

SB-060-09		24-090		WI-190-SB	
depth (km)	velocity (km/s)	depth (km)	velocity (km/s)	depth (km)	velocity (km/s)
0.0	4.0	0.0	4.0	0.0	3.7
2.0	4.0	1.5	4.0	3.5	3.7
2.0	6.0	1.5	6.0	3.5	6.0
17.0	6.0	18.5	6.0	16.0	6.0
17.0	6.1	18.5	6.2	16.0	6.1
19.5	6.3	21.5	6.3	21.0	6.1
21.0	6.9	23.0	6.9	21.0	7.2
25.0	7.4	26.0	7.3	25.0	8.1
25.0	8.0	26.0	8.0		

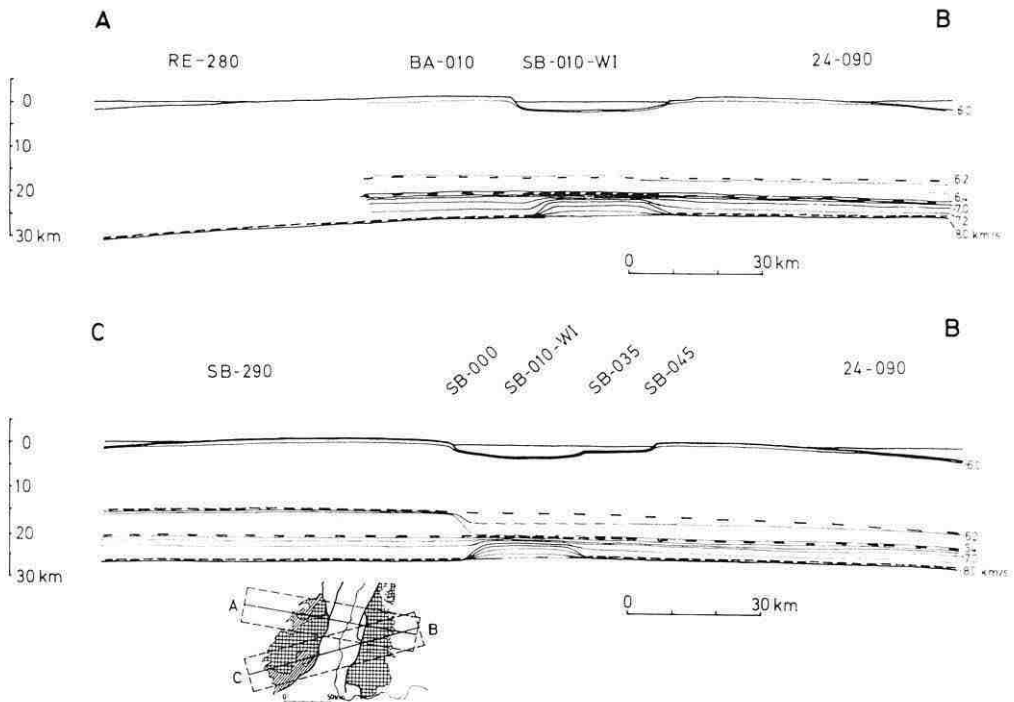| LT-225		BA-010 model 1		model 2		16-195	
depth (km)	velocity (km/s)	depth (km)	velocity (km/s)	depth (km)	velocity (km/s)	depth (km)	velocity (km/s)
0.0	4.0	0.0	4.0	0.0	4.0	0.0	4.0
3.0	4.0	0.8	4.0	0.8	4.0	5.0	4.0
3.0	6.0	0.8	6.0	0.8	6.0	5.0	6.1
17.5	6.0	17.5	6.0	7.0	6.0	14.0	6.1
17.5	6.1	17.5	6.3	9.5	5.5	14.0	6.4
21.5	6.3	21.0	6.3	12.5	5.5	23.0	6.4
22.5	6.8	21.5	6.9	13.5	6.2	24.0	6.75
26.0	7.4	25.5	7.3	19.5	6.2	29.0	7.0
26.0	8.0	25.5	7.9	20.5	6.9	29.0	7.9
				25.5	7.4		
				25.5	7.9		

Fig. 16. Crustal sections through the southern part of the Rhinegraben. Thin lines: lines of equal velocity, contour interval 0.2 km/s. Thick continuous line: surface of the crystalline basement. Thick dashed lines: mean depth of the main crustal boundaries

which apparently represents a fairly active stage of epeirogeny (Menard, 1973) is culminating in the southernmost part of the Rhinegraben from where the elevation of the apex is slightly dipping towards the north. For the northern part of the graben proper Meissner and Vetter (1974) deduce a similar structure of the lower crust. They find a velocity of 7.2—7.4 km/s and a strong velocity gradient at a depth of 24 to 25 km in the graben proper. Here $P_M P$-reflections (our phase 1) are also not observed, while the phase with 7.2—7.4 km/s (our phase 2) evidently is absent outside the graben.

A P_n-velocity of 8.2 km/s is reported by Hirn and Perrier (1974) on reversed profiles in the Limagne graben parallel to its strike at a depth of 40 km. They also find a velocity range of 7.2—7.4 km/s between a depth of 20 to 25 km from where the velocity increases continuously to that of the upper mantle.

From seismic reflection measurements, Dohr (1967, 1970) reports reflections with traveltimes of 7 s and 8.5 to 9.0 s which can be attributed to the zone of strong velocity gradient at about 21 km depth and to the depth range at about 25 km. The reflections observed with traveltimes of 13.5 s and about 17.5 s may indicate zones of strong heterogeneities within the upper mantle. Recent long-range observations in France (Hirn *et al.*, 1973) and similar observations by Emter (1971) under the Swabian Jura about 80 to 100 km east of the graben proper have shown the existence of pronounced heterogeneities in the lower lithosphere. However, as already mentioned by Rhine-
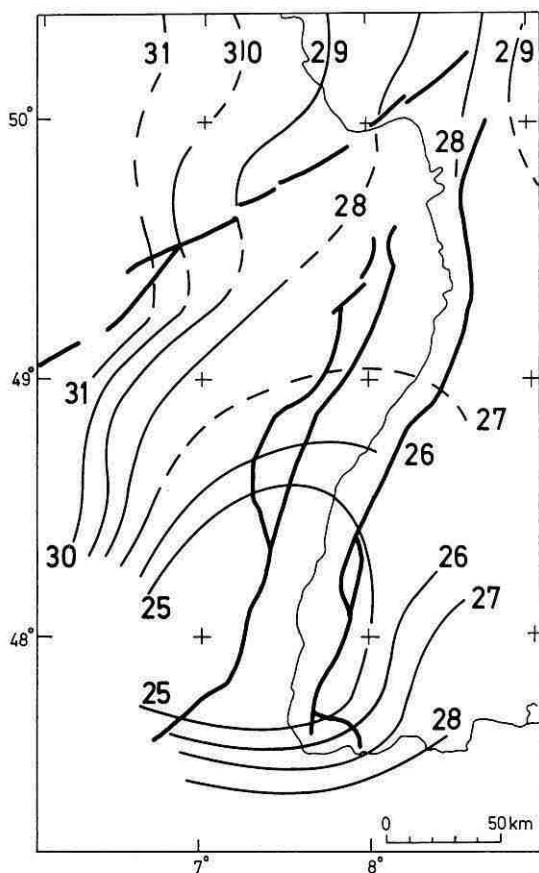
Fig. 17. Contour map of the depth to the crust-mantle boundary combining the map of Fig. 10 and the map shown by Meissner and Vetter (1974, Fig. 5). 28 depth in km

graben Research Group (1974), at present no long-range data in the graben area are available which would allow a statement about the deeper structure below the crust-mantle boundary.

The contour map of the heat-flow anomaly (Haenel, 1971) and the geoid undulations (Groten and Rummel, 1974) reflect the elevated and anomalous crust-mantle transition in the southern part of the Rhinegraben. A low-resistivity layer of 25—30 Ωm is deduced inside the graben from geomagnetic (Winter, 1973, 1974) and magneto-telluric (Scheelke, 1974) observations at a depth of about 25 km which is not encountered at a distance of 45 km outside the graben (Haak and Reitmayr, 1974). These findings are supported by estimates of temperatures at a depth of 25 km in the Rhinegraben area (Mueller and Rybach, 1974). Values of 660 °C are found below the graben proper which exceed the temperatures below the Black Forest by 200 °C at the same depth. These results suggest again that the anomalous crust-mantle transition is confined to the graben proper.

In conclusion, the seismic investigations of the Rhinegraben rift system have established a detailed model of the crust and upper mantle in this area which differs

specificly from the neighbouring normal continental crust. A highly anomalous crust-mantle transition confined to the graben proper is superimposed on a regional uplift of the crust-mantle boundary.

The difference of velocity-depth models at the crust-mantle boundary within the graben proper and below the flanks suggests strongly that the lower crust and upper mantle below the Rhinegraben proper have a different composition than below the adjacent areas. The disappearance of the first-order discontinuity and the modification of the velocity gradient in the lower crust, both phenomena strictly confined to the graben, cannot be explained by heating and/or depressurization from local uplift. Mass intrusion from the upper mantle, differentiation, or phase transformations can be considered as possible causes for the observed phenomena.

References

Ansorge, J., Emter, D., Fuchs, K., Lauer, J. P., Mueller, St., Peterschmitt, E.: Structure of the crust and upper mantle in the rift system around the Rhinegraben. In: Illies, H., Mueller, St. (eds.): Graben Problems, pp. 190–197. Stuttgart: Schweizerbart 1970

Bamford, D.: Refraction data in western Germany — a time-term interpretation. Z. Geophys. *39*, 907–927, 1973

Demnati, A., Dohr, G.: Reflexionsseismische Tiefensondierungen im Bereich des Oberrheintalgrabens und des Kraichgaues. Z. Geophys. *31*, 229–245, 1965

Dix, C. H.: Seismic velocities from surface measurements. Geophysics 20, 68–86, 1955

Dohr, G.: Zur reflexionsseismischen Erfassung sehr tiefer Unstetigkeitsflächen. Erdöl, Kohle *10*, 278–281, 1957

Dohr, G.: Beobachtungen von Tiefenreflexionen im Oberrheingraben. Abh. Geol. Landesamt Baden-Württemberg *6*, 94–95, 1967

Dohr, G.: Reflexionsseismische Messungen im Oberrheingraben mit digitaler Aufzeichnungstechnik und Bearbeitung. In: Illies, H., Mueller, St. (eds.): Graben Problems, pp. 207–218. Stuttgart: Schweizerbart 1970

Emter, D.: Ergebnisse seismischer Untersuchungen der Erdkruste und des obersten Erdmantels in Südwestdeutschland. Dissertation, Univ. Stuttgart, 108 p., 1971

Förtsch, O.: Analyse der seismischen Registrierungen der Großsprengung bei Haslach im Schwarzwald am 28. April 1948. Geol. Jahrb. *66*, 65–80, 1951

German Research Group for Explosion Seismology: Crustal structure in western Germany. Z. Geophys. *30*, 209–234, 1964

Giese, P., Stein, A.: Versuch einer einheitlichen Auswertung tiefenseismischer Messungen aus dem Bereich zwischen der Nordsee und den Alpen. Z. Geophys. *37*, 237–272, 1971

Groten, E., Rummel, R.: Improved gravimetric geoid for $7° \leq \lambda \leq 12°$ (E) and $48° \leq \phi \leq 54°$ (N). Allgem. Vermessungsnachr., in press, 1974

Haak, V., Reitmayr, G.: The distribution of electrical resistivity in the Rhinegraben area as determined by telluric and magnetotelluric methods. In: Illies, H., Fuchs, K. (eds.): Approaches to Taphrogenesis, pp. 366–369. Stuttgart: Schweizerbart 1974

Haenel, R.: Bestimmungen der terrestrischen Wärmestromdichte in Deutschland. Z. Geophys. *37*, 119—134, 1971

Hirn, A., Perrier, G.: Deep seismic sounding in the Limagne graben. In: Illies, H., Fuchs, K. (eds.).: Approaches to Taphrogenesis, pp. 329—340. Stuttgart: Schweizerbart 1974

Hirn, A., Steinmetz, L., Kind, R., Fuchs, K.: Long range profiles in western Europe: II. Fine structure of the lower lithosphere in France (southern Bretagne). Z. Geophys. *39*, 363—384, 1973

Landisman, M., Mueller, S.: Seismic studies of the earth's crust in continents. II.: Analysis of wave propagation in continents and adjacent shelf areas. Geophys. J. *10*, 539—554, 1966

Lauer, J. P., Peterschmitt, E.: Ondes réfléchies des explosions des Bagenelles et de St. Nabor (Vosges, France). Proc. 10th Gen. Ass. Europ. Seismol. Comm. (Leningrad 1968) Acad. Sciences USSR, Moscow, 444—453, 1970

Meissner, R., Berckhemer, H.: Seismic refraction measurements in the northern Rhinegraben. Abh. Geol. Landesamt Baden-Württemberg *6*, 105—108, 1967

Meissner, R., Berckhemer, H., Wilde, R., Poursadeg, M.: Interpretation of seismic refraction measurements in the northern part of the Rhinegraben. In: Illies, H., Mueller, St. (eds.): Graben Problems. pp. 184—190. Stuttgart: Schweizerbart 1970

Meissner, R., Vetter, U.: The northern end of the Rhinegraben due to some geophysical measurements. In: Illies, H., Fuchs, K. (eds.): Approaches to Taphrogenesis, pp. 236—243. Stuttgart: Schweizerbart 1974

Menard, H. W.: Epeirogeny and plate tectonics. EOS Trans. AGU *54*, 1244—1255, 1973

Mueller, St., Landisman, M.: Seismic studies of the earth's crust in continents. I.: Evidence for a low-velocity zone in the upper part of the lithosphere. Geophys. J. *10*, 525—538, 1966

Mueller, St., Peterschmitt, E., Fuchs, K., Ansorge, J.: The rift structure of the crust and the upper mantle beneath the Rhinegraben. Abh. Geol. Landesamt Baden-Württemberg *6*, 108—113, 1967

Mueller, St., Peterschmitt, E., Fuchs, K., Ansorge, J:. Crustal structure beneath the Rhinegraben from seismic refraction and reflection measurements. Tectonophysics *8*, 529—542, 1969

Mueller, St., Peterschmitt, E., Fuchs, K., Emter, D., Ansorge, J.: Crustal structure of the Rhinegraben area. In: Mueller, St. (ed.): Crustal structure based on seismic data. Tectonophysics *20*, 381—392, 1973

Mueller, St., Rybach, L.: Crustal dynamics in the central part of the Rhinegraben. In: Illies, H., Fuchs, K. (eds.): Approaches to Taphrogenesis, pp. 379—388. Stuttgart: Schweizerbart 1974

Prodehl, C.: Struktur der tieferen Erdkruste in Südbayern und längs eines Querprofiles durch die Ostalpen, abgeleitet aus refraktionsseismischen Messungen bis 1964. Boll. Geofis. Teor. Appl. *7*, 35—88, 1965

Reich, H., Schulz, G. A., Förtsch, O.: Das geophysikalische Ergebnis der Sprengung von Haslach im südlichen Schwarzwald. Geol. Rundschau *36*, 85—96, 1948

Rhinegraben Research Group for Explosion Seismology: The 1972 seismic refraction experiment in the Rhinegraben. — First results. In: Illies, H., Fuchs, K. (eds.): Approaches to Taphrogenesis, pp. 122—137. Stuttgart: Schweizerbart 1974

Rothé, J. P.: Quelques expériences sur la structure de la croûte terrestre en Europe occidentale. In: Ingerson, E.: (ed.) Contributions in Geophysics in Honor of Beno Gutenberg, pp. 135—151. Oxford: Pergamon Press 1958

Rothé, J. P., Peterschmitt, E.: Étude sismique des explosions d'Haslach. Ann. Inst. Phys. Globe Strasbourg *5,3*, 3—28, 1950

Scheelke, I.: Models for the resistivity distribution from magneto-telluric soundings. — In: Illies, H., Fuchs, K. (eds.): Approaches to Taphrogenesis, pp. 362—365, Stuttgart: Schweizerbart 1974

Schulz, G.: Reflexionen aus dem kristallinen Untergrund des Pfälzer Berglandes. Z. Geophys. *23*, 225—235, 1957

Stewart, S. W.: Seismic ray theory applied to refraction surveys of the earth's crust in Missouri. Ph. D. Thesis, St. Louis University, St. Louis, Missouri, USA, 189 p., 1966

Winter, R.: Der Oberrheingraben als Anomalie der elektrischen Leitfähigkeit, untersucht nit Methoden der erdmagnetischen Tiefensondierung. Diss., Univ. Göttingen, 117 p., 1973

Winter, R.: A model for the resistivity distribution from geomagnetic depth soundings. In: Illies, H., Fuchs, K. (eds.): Approaches to Taphrogenesis, pp. 369–375. Stuttgart: Schweizerbart 1974

J. B. Edel
Institut de Physique du Globe
5, rue René Descartes
F-67 Strasbourg
France

K. Fuchs
C. Gelbke
C. Prodehl
Geophysikalisches Institut
der Universität
D-7500 Karlsruhe, Hertzstr. 16
Federal Republic of Germany